

**DETECTION LIMITS FOR SILICATES IN RAMAN SPECTRA OF MIXTURES WITH VOLCANIC GLASS.** Genesis Berlanga<sup>1</sup>, M. Darby Dyar<sup>2</sup>, Laura Breitenfeld<sup>2</sup>, Carlie Wagoner<sup>2</sup>, Avery Hanlon<sup>2</sup>, Paul Bartholomew<sup>3</sup>, Shiv K. Sharma<sup>1</sup>, and Anupam K. Misra<sup>1</sup>. <sup>1</sup>Univ. of Hawai'i Manoa, Hawai'i Inst. of Geophysics and Planetology, 1680 East-West Rd., Honolulu, HI 96822, gberlang@hawaii.edu, <sup>2</sup>Mount Holyoke Col., Dept. of Astronomy, 50 College St., South Hadley, MA 01075, <sup>3</sup>Dept. of Biology and Environmental Science, Univ. of New Haven, West Haven, CT 06516.

**Introduction:** The *Mars 2020* mission will employ two different Raman instruments to probe the surface of Mars. SHERLOC will utilize deep ultraviolet (DUV) resonance to scan habitable environments with both Raman and luminescence for organics and chemicals [1]. Super-Cam will probe Mars surface materials at distances up to 12 m [2]. SuperCam will use a gated laser system to mitigate contributions from fluorescence, while SHERLOC has an ungated, continuous wave system to enhance signal return.

The choice of time-resolved vs. standard (ungated) systems may be critically important to the success of these instruments, though the extent to which fluorescence [3-5] will be encountered in Mars samples is unknown. Terrestrial Raman spectral libraries are largely ungated, and thus contaminated by mild to strong fluorescence features resulting from organics, rare earth, or transition metals that give rise to fluorescence centers. These fluorescent features are not characteristics of the individual minerals, but of the fluorescing species themselves. Contaminated spectra are usually ignored and discarded in laboratory studies because they are poorly understood. But if fluorescence effects are observed in data from Mars (and other bodies where Raman landers have been proposed), then they must be managed and understood.

A second issue confronting practical implementation of remote Raman systems relates to the analysis of mixtures of minerals. Only very limited data on mixtures exist for Raman spectroscopy [6,7]. Studies of mineral/glass detection limits by our group [8,9] under Venus conditions used only a single unspecified synthetic glass matrix measured by a single gated Raman system.

This project builds upon our previous work by exploring mineral detection limits in the context of the choice of gating vs. continuous Raman. We vary the laser system, matrix composition, and mineral proportions, employing common volcanic silicate minerals in naturally-occurring volcanic glasses with compositions directly analogous to those that might be found on the surfaces of terrestrial bodies in our solar system.

**Samples studied:** This project employed mixtures of seven different phases in varying proportions. Volcanic glasses from a rhyolitic volcano in Mexico (locality unknown, but likely the Tequila Volcano) and Kilauea Volcano in Hawai'i were selected to represent extremes of possible glass composition, with  $\text{SiO}_2 = 75.68$

and 51.56, respectively [10]. Minerals were chosen to be typical components of igneous rocks, and included forsterite (olivine) from the classic locality at San Carlos, NM; augite (clinopyroxene) from the Harcourt Graphite Mine, Cardiff Township, Haliburton Co., Ontario; diopside (clinopyroxene) from Hershel Ontario (Canada); bytownite (plagioclase feldspar) from Crystal Bay, Minnesota; and labradorite (plagioclase) from Chihuahua, Mexico [11].

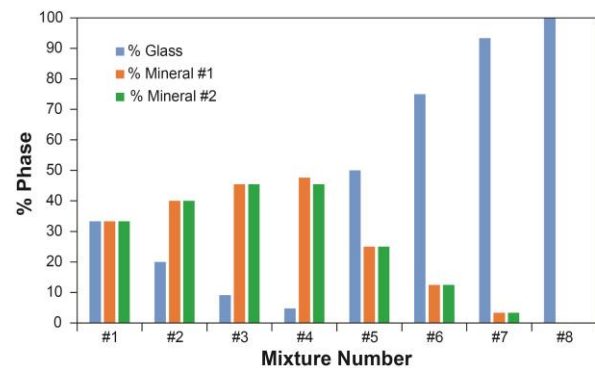


**Figure 1.** Volume proportions of phases used in mixtures. Glass was either basaltic (Hawai'i) or rhyolitic (Mexico) [10] and the minerals were binary combinations of labradorite, bytownite, augite, diopside, or forsterite [11] except for the pure glasses ("mixture" #8).

Using known compositions [1,2], densities of all phases were calculated. Glass and minerals were ground and sieved to grain sizes between 38 and 63  $\mu\text{m}$  prior to weighing into mixtures. Mixtures with several different volume proportions were created (Figure 1). Spectra of pure phases (minerals and glasses) were also acquired.

**Methods:** Raman data were acquired on two different instruments. One set of spectra was acquired on a Bruker Optics, Inc. BRAVO Raman spectrometer,

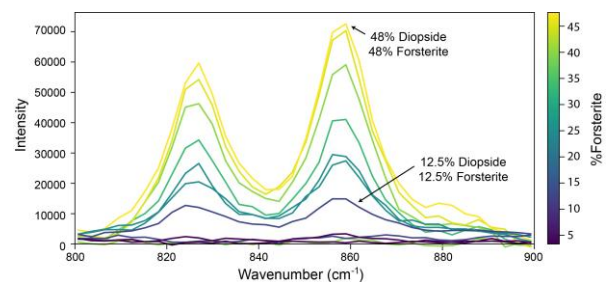


**Figure 2.** Close-up of the olivine peaks in volume proportions of mixtures of diopside and forsterite in Mexico glass. Olivine is detected easily in the 12.5% mixtures.

which uses dual laser (758 and 852 nm) excitation and a patented fluorescence mitigation strategy involving successive heating of the laser [12]. With a scan time of 10s and wavenumber range of 300-3350  $\text{cm}^{-1}$ , each sample was run three times and the spectra were averaged. The BRAVO produces baseline-subtracted data. Samples were run in glass vials; comparisons of in-vial spectra with direct powders of the same samples showed no significant differences. The signal is not gated.

The second set of data was acquired on the exact same set of samples. The homebuilt remote Raman-LIBS-LIF system in the Raman Spectral Laboratory at the Hawai'i Institute of Geophysics and Planetology, University of Hawai'i-Manoa, was used. The system employs a 532 nm pulsed laser (10 mJ/pulse, 10 ns pulse width) with a laser repetition rate of 15 Hz and can be gated to mitigate fluorescence. A Kaiser Optical Systems stacked, two-trace, volume phase holographic grating (532-616 nm and 606-702 nm range) was used to cover the entire Raman range (90-4500  $\text{cm}^{-1}$ ) with a resolution of 10  $\text{cm}^{-1}$ . Sample powders were taken out of the vials and placed on an anodized aluminum plate. A 5 mm laser spot size was used and entirely contained within the sample. All samples were run identically using 5s exposures, 15 laser pulses/s, with a gate width of 20 ns, at a 10 m distance. Data were background subtracted and wavelength calibrated with internal barite, sulfur, and cyclohexane standards.

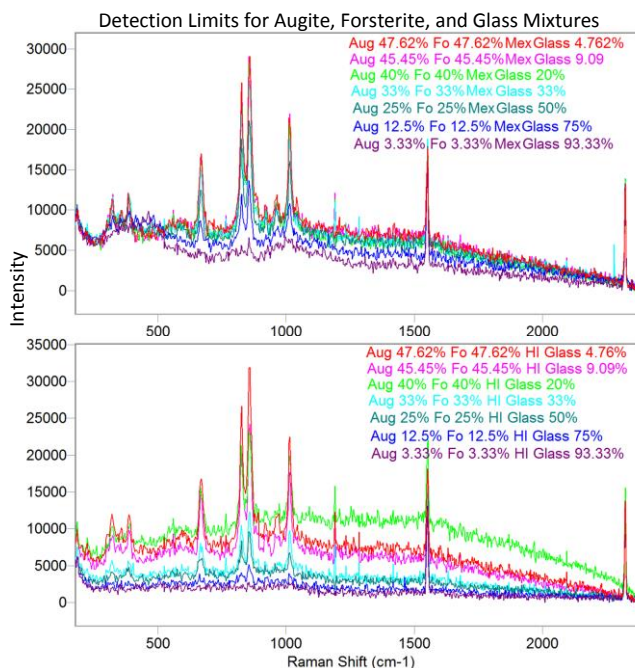


**Figure 3.** Comparison of detection limits for augite, forsterite, and glass mixtures ranging from 3.3 – 48% by volume using Hawai'i (HI) basaltic glass and Mexico (Mex) rhyolitic glass.

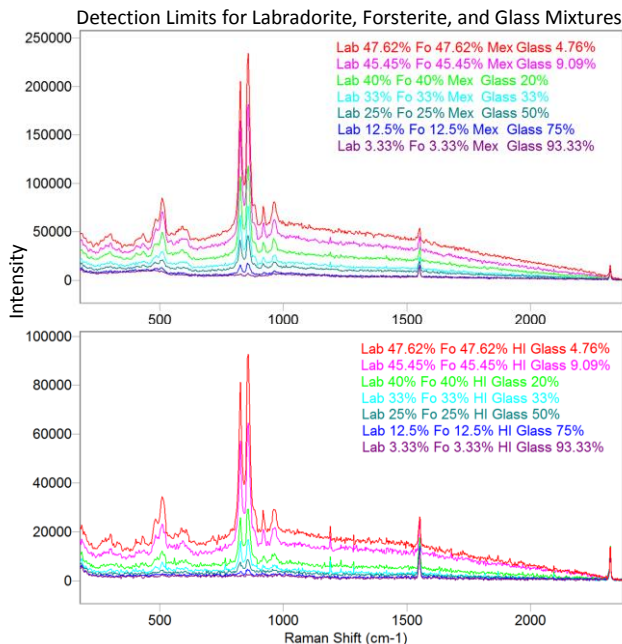


**Figure 4.** Comparison of detection limits for labradorite, forsterite, and glass mixtures ranging from 3.3-48% by volume, using Hawai'i (HI) basaltic glass and Mexico (Mex) rhyolitic glass.

**Results:** Figures 3 and 4 demonstrate that some phases can be detected at 3.3% abundances by volume. In those data, it is still possible to determine the composition of olivine through the observed Raman peaks at 822, 854, 880, and 916  $\text{cm}^{-1}$  [13]. Augite is observed at 328, 395, 666, and 1011  $\text{cm}^{-1}$ . Labradorite is observed as a doublet at 481 and 509  $\text{cm}^{-1}$ . Oxygen and nitrogen Raman peaks are observed at 1556 and 2331  $\text{cm}^{-1}$ . Raman peaks were more easily distinguished in rhyolitic Mexico glass mixtures than in basaltic Hawai'i glass mixtures.

**Conclusions:** Mineral and glass mixtures were measured through standard (ungated) and time-resolved Raman systems. Detection limits were investigated for common terrestrial planet igneous minerals mixed with rhyolitic or basaltic glasses. Most mineral phases were identifiable at a 3.3-12.5% abundance by volume.

**Acknowledgments:** Research supported by the NASA RISE SSERVI, the Massachusetts Space Grant Consortium, NASA EPSCoR, NASA PICASSO, and the SuperCam program under NASA Mars 2020.

**References:** [1] Beegle L. W. et al. (2014) *11th Intl. GeoRaman Conf.*, Abstract #5101. [2] Maurice S. et al. (2015) *LPS XLVI*, Abstract #2818. [3] Bartholomew P.R. (2012) *GSA Abstr.* 44, 622. [4] Jaszczak J.A. (2013) *Rocks Mins.*, 88, 184-189. [5] Carron K. and Cox R. (2010) *Anal. Chem.*, 82, 3419-3425. [6] Breitenfeld L. et al. (2016) *Lunar Planet. Sci. XLVII*, Abstract #2186. [7] Breitenfeld L. et al. (2016) *Lunar Planet. Sci. XLVII*, Abstract #2430. [8] Sharma S. K. et al. (2011) *LPS XLII*, Abstract #1250. [9] Clegg S. M. et al. (2014) *Appl. Spectrosc.*, 68, 925-936. [10] Mackie J. et al. (2017) *LPS XLVIII*, Abstract #1292. [11] Byrne S. A. et al. (2015) *LPS XLVI*, Abstract #1499. [12] Cooper J. B. et al. (2014) *Spectrosc.*, 29, 38-42. [13] Breitenfeld L. et al. (2017) *LPSC XLVIII*, Abstract #1898..